Articles in PresS. Am J Physiol Lung Cell Mol Physiol (October 30, 2009). doi:10.1152/ajplung.00064.2009

Bone Marrow-Derived Progenitor Cells Prevent Thrombin-Induced Increase in Lung Vascular Permeability

Yidan D. Zhao*, Hiroshi Ohkawara*, Stephen M. Vogel, Asrar B. Malik and You-Yang Zhao

Department of Pharmacology and Center for Lung and Vascular Biology, University of Illinois College of Medicine, Chicago, Illinois

*, Contributed equally

Running head: BMPC prevent endothelial barrier dysfunction

Address correspondence to:

You-Yang Zhao or Yidan D. Zhao

Department of Pharmacology

Center for Lung and Vascular Biology

University of Illinois College of Medicine

835 S. Wolcott Ave., Rm. E403-MSB (MC 868)

Chicago, IL 60612

Phone: 312-355-0238; Fax: 312-996-1225; E-mail: yyzhao@uic.edu (YY Zhao)

Phone: 312-996-5892; Fax: 312-996-1225; E-mail: yidan@uic.edu (YD Zhao).

Abbreviations: AJs, adherens junctions; BMPCs, bone marrow-derived progenitor cells; ECs, endothelial cells; MLC, myosin light chain; PAR-1, protease-activated receptor-1; TER, transendothelial monolayer electric resitance; VE-cadherin, vascular endothelial cadherin.

Abstract

Since thrombin activation of endothelial cells (ECs) is well known to increase endothelial permeability by disassembly of adherens junctions (AJs) and actino-myosin contractility mechanism involving myosin light chain (MLC) phosphorylation, we investigated the effects of bone marrow-derived progenitor cells (BMPCs) on the thrombin-induced endothelial permeability response. We observed that addition of BMPCs to endothelial monolayers at a fixed ratio prevented the thrombin-induced decrease in transendothelial electrical resistance, a measure of AJ integrity, and increased mouse pulmonary microvessel filtration coefficient, a measure of transvascular liquid permeability. The barrier protection was coupled to increased VE-cadherin expression and increased Cdc42 activity in ECs. Using siRNA to deplete Cdc42 in ECs, we demonstrated a key role of Cdc42 in signaling the BMPC-induced endothelial barrier protection. Endothelial integrity induced by BMPCs was also secondary to inhibition of MLC phosphorylation in ECs. Thus, BMPCs interacting with ECs prevent thrombin-induced endothelial hyper-permeability by a mechanism involving AJ barrier annealing, inhibition of MLC phosphorylation, and activation of Cdc42.

Key Words: adherens junctions, Cdc42; VE-cadherin, myosin light chain.

Introduction

Bone marrow-derived progenitor cells (BMPCs) positive for antigen markers CD34 and Flk-1 contribute to angiogenesis at sites of neovascularization (2, 11, 24). Recruitment and engraftment of BMPCs may be required for formation of new blood vessels (2, 11, 18, 21, 24). These published studies suggest that BMPC transplantation is a potential therapeutic strategy of neovascularization for ischemic diseases (10, 22, 23). Several studies have also demonstrated the protective role of mesenchymal stem cells in experimental models of acute lung injury (8, 16). We have recently shown BMPC-mediated endothelial barrier protection in the sepsis model of acute lung injury through sphingosine-1-phosphate signaling (31). To address whether the BMPC effects on the endothelium could be extended to other pro-inflammatory mediators, here we investigated the effects of BMPCs in mitigating increase in endothelial permeability induced by the archetypal mediator thrombin. Thrombin ligation of protease-activated receptor-1 (PAR-1) increases endothelial permeability secondary to disassembly of adherens junctions (AJs) and phosphorylation of myosin light chain (MLC) (28). Loss of vascular endothelial cadherin (VE-cadherin) homotypic interaction induced by thrombin results in increased endothelial permeability (9, 12, 17).

Using mouse BMPCs positive for CD133 and CD34, we observed that BMPCs interacting with pulmonary microvascular endothelial cells (ECs) prevented the thrombin-induced increase in endothelial permeability. The endothelial barrier protection was secondary to inhibition of MLC phosphorylation and strengthening of the AJ barrier through activation of the RhoGTPase Cdc42.

Materials and Methods

Mice. All mice were bred and maintained in the University of Illinois facility according to NIH guidelines. Approval for animal care and use in these experiments was granted by the Animal Care and Use Committee.

Mouse bone marrow-derived progenitor cells. Mouse BMPCs were isolated using modification of methods in (29-31). Briefly, the femur and tibia were stripped from muscle and connective tissue, bone was cut at both ends, and bone marrow was flushed with HBSS using syringe with a 25gauge needle. The bones were cut into small pieces and incubated with 10 mL of collagenaseA solution (1.0 mg/mL in HBSS) in 50 ml tube for 3-4 min at 37^{o}C with gentle shaking. The digested mixtures together with the initial bone marrow HBSS flush were filtered using a 40μm nylon filter. Mononuclear cells were isolated by density gradient (Ficoll-Paque, Amersham) following centrifugation at 1600rpm for 30 min. The cells were re-suspended in EBM-2MV endothelial culture media using the supplement kit (Lonza) made 10% FBS, 50 U/ml penicillin and streptomycin, 2 mmol/l L glutamine (Invitrogen), and additional VEGF (5ng/ml). The cells were then plated onto fibronectin-collagen-gelatin (ratio 1:1:1)-coated tissue culture flasks. The cells were incubated for 48 h at 37°C with 5% CO_2 at which time the non-adherent cells, representing 90-95% of the initial culture, were washed away. The adherent cells were then cultured for 21 d. The phenotype of confluent cell population was assessed by determining the expression of protein markers described below using FACS analysis.

BMPC transplantation. BMPCs ($3x10^5$ BMPCs in 200 μl of EBM-2MV medium) were injected through external jugular vein.

FACS analysis. Following 21 d in culture, BMPCs were detached with 1 mmol/L EDTA in PBS and fixed with 100μl of 4% paraformaldehyde at room temperature for 10 minutes. The

cells were then centrifuged for 5 minutes and the supernatant was aspirated. The cells were then incubated with the following antibodies in dark at room temperature for 30 minutes: phycoerythrin-labeled anti-Sca1 (BD PharMingen), allophycocyanin-labeled anti-CD34 antibodies (BD PharMingen), goat anti-CD31 (PharMingen), mouse anti-CD133 (BD PharMingen), and rabbit anti-VE-cadherin (Santa Cruz). Rabbit anti-mouse or goat anti-rabbit conjugated with FITC (Vector) or Alexa Fluor-labeled anti-goat 594 (Invitrogen) were used as the secondary antibody. The labeled cells were then washed with PBS and resuspended in 0.5ml of 1 mmol/L EDTA in PBS to prevent aggregation and analyzed with Coulter Elite ESP (Beckman-Coulter). The experiment was done in triplicate and repeated twice.

Colony forming units (CFU-C) assay. Clonogenic assays were performed using either bone marrow-derived cells or lung microvascular ECs and mixture of MethodCult RH4100 (StemCell Technologies) with EBM-2MV medium (1:1) with 5% FBS. Cell-plating densities for CFU-C assays were optimized according to manufacture's suggestion at a density of 10^3 cells/well of 6-well plate in 3 mL complete EBM-2MV medium containing 5% FBS and 2 X of the supplement, and addition of 50 U/ml penicillin and streptomycin, 2 mmol/L L-glutamine, and additional VEGF (5ng/ml).Colonies were identified as large, often irregular, multicentric colonies and scored at 18 d following the manufacture instructions. After 18 d incubation, the colonies from BM-derived cells were collected and re-plated into chamber slides and cultured for another 2 days. They were then fixed and immunostained with antibodies against CD133 and CD34 according to the protocol supplied with MethodCult RH4100 kit.

Mouse lung microvascular ECs. Primary cultures of mouse lung microvascular ECs were established using cells immunoselected from lungs of 4-5 week old mice as described (26). Briefly, ECs were selected using a rat antibody to mouse CD-31 (BD Pharmingen) and secondary

antibody coupled to immunomagnetic beads (Dynabeads M-450; Dynals). The rosetted cells were then isolated and washed using a magnetic particle concentrator (Dynal MPC-15; Dynals). Purified ECs were plated onto 6-well plates coated with 0.2% gelatin (Sigma-Aldrich) in EBM-2MV complete medium (Lonza) with 10% FBS (Invitrogen). These primary ECs were used at passages 3-4 for all experiments.

Transendothelial electrical resistance (TER). Endothelial junctional barrier function was determined by measuring real-time changes in TER (25). ECs were seeded on a gelatin-coated gold electrode ($5.0x10^4$ cells/cm^2), grown to confluence to allow adherens junctions (AJs) to form. Changes in TER in response to human alpha-thrombin (Enzyme Research Laboratories) were monitored for up to 6 h. The small electrode and the larger counter-electrode were connected to a phase-sensitive lock-in amplifier. A constant current of 1 μA was supplied by a 1-V, 4000-Hz AC signal connected serially to a 1-MΩ resistor between the small electrode and larger counter-electrode. The voltage was monitored by a lock-in amplifier, stored, and processed by a personal computer. The same computer controlled the amplifier output and switched the measurement to different electrodes in the course of an experiment. Data are presented as changes in the resistive portion of resistance normalized to its value at time zero.

Pulmonary uptake of BMPCs. BMPCs were labeled with rhodamine red fluorophore (CMTMR, Molecular Probes). In each case after injection of $3x10^5$ labeled cells into the external jugular vein, the mice were sacrificed at day 4. The location of BMPCs within the mouse lung microvasculature counterstained with VE-cadherin was identified by confocal microscopy. In other studies, $3x10^5$ BMPCs labeled with ^{111}Indium oxine as described for leukocytes (5) were injected into mice to determine their organ specific uptake using a gamma counter (Packard Instruments).

Immunofluorescence. Cells and sections of peripheral lung tissue were fixed for 10 min at RT with PBS made 4% formaldehyde, permeabilized for 30 min in Triton X-100 (0.5% in PBS), and incubated with 5% non-fat skim milk in PBS for 90 min. Cells and sections were incubated for 180 min at room temperature with anti-VE-cadherin antibody (Santa Cruz) or anti-Cdc42 (Santa Cruz) antibody, and stained with fluorescein isothiocyanate (FITC)-conjugated second antibody (Chemicon). Stained cells and sections were visualized with Zeiss LSM 510 confocal microscope.

Triton X-100 solubility. Cell extracts were separated into Triton X-100-soluble and -insoluble fractions according to published protocol (14). Samples were initially homogenized in extraction buffer I made 1% Triton X-100, 1% NP-40, 10 mmol/L Tris-HCl, and 150 mmol/L NaCl (TBS) with 2 mmol/L $CaCl_2$, pH 7.5, and protease inhibitors. Extracts were centrifuged at 12,000 x *g* for 5 min at 4°C to separate Triton X-100-soluble from -insoluble fractions. This supernatant was considered the Triton X-100-soluble fraction. After the first extraction, the pellets were gently washed three times in TBS containing protease inhibitors and then re-suspended in the same volume of Triton X-100 supernatant and homogenized in extraction buffer II made 0.5% SDS, 1% NP-40, and TBS with protease inhibitors. Extracts were centrifuged at 12,000 x *g* for 5 min at 4°C; this supernatant was considered the Triton X-100–insoluble fraction. The Triton X-100 – insoluble protein fractions and total protein were used for immunobloting.

Immunoblotting. Protein concentrations were determined using the BCA protein assay (Pierce). Equal amounts of the protein lysates were separated by SDS-PAGE and transferred onto nitrocellulose membranes. The membranes were incubated for 180 min at RT with the following antibodies: anti-VE-cadherin (1:1000, Santa Cruz), anti-RhoA (1:100, Santa Cruz), anti-Cdc42 (1:1000, Santa Cruz), anti-Thr18/Ser19 MLCp (1:500, Cell Signaling) and anti-MLC

(1:1000, Cell Signaling). After washed with TBS-Tween, the blots were incubated for 60 min at RT with horseradish peroxidase-conjugated antibodies, respectively: anti-goat (1:15,000; Santa Cruz) for VE-cadherin; anti-mouse IgG (1:15,000; Santa Cruz) for RhoA; anti-rabbit (1:15,000; Sigma-Aldrich) for Cdc42, MLCp, and MLC. Signals from immunoreactive bands were visualized by fluorography using an ECL reagent (Pierce). The intensity of individual bands in immunoblots were quantified using the NIH IMAGE program.

Actin stress fiber formation. Content of actin stress fibers was determined in confluent ECs grown in a slide chamber (Nalge Nunc International). Cells were washed with PBS, fixed in 4% formaldehyde/PBS for 15 min, and permeabilized for 5 min at RT in Triton X-100 (0.05% in PBS). Cells were stained for 90 min with 1 μg/ml tetramethylrhodamine isothiocyanate (TRITC)-phalloidin in PBS. Stained ECs were analyzed by confocal microscopy.

RhoGTPase activity assay. The GTP-bound active forms of RhoA and Cdc42 were determined by pull-down assays (1, 12). Cells were washed with ice-cold PBS five times and lysed in lysis buffer (50 mmol/L Tris, pH 7.4, 1% Triton X-100, 0.5% sodium deoxycholate, 0.1% SDS, 500 mmol/L NaCl, 10 mmol/L $MgCl_2$, 10 μg/ml each of aprotinin and leupeptin, and 1 mmol/L phenylmethylsulfonyl fluoride). After centrifugation at 18,000 x *g* at 4°C for 2 min, the extracts were incubated at 4°C for 60 min with glutathione-sepharose beads coupled with glutathione-S-transferase (GST)-rhotekin fusion protein for determination of Rho activity or GST-p21-activated kinase (PAK) for determination of Cdc42 activity. Bound RhoA and Cdc42 proteins were quantified by Western blotting as described above.

Transfection of siRNA. siRNA were transduced in ECs by electroporation using the basic endothelial cell nucleofactor kit (VPI-1001, Lonza) with the Amaxa nucleofactor device (Lonza). Briefly, mouse lung microvascular ECs, at 60% confluency, were trypsinized, mixed with 5μg

siRNA to Cdc42 or control non-silencing siRNA along with 100 µl of transfection solution. Cells were electroporated by Amaxa nucleofactor device using the manufacturer's recommended program (S-005). At 24 h after transfection, the culture medium was changed.

Pulmonary microvascular permeability. Mice (n=8) were injected intravenously with $0.3x10^6$ BMPCs or ECs (in 200 µl of EBM-2 medium) through the external jugular vein. Mice were sacrificed 4d after BMPC or EC injection to determine the lung microvascular filtration coefficient ($K_{f,c}$) and final lung wet-to-dry weight ratio measurements. $K_{f,c}$ was measured to determine pulmonary microvascular permeability (28). The lung preparations were ventilated and perfused with RPMI-1640 (Invitrogen) at constant flow. The rate of weight gain for a given increase in capillary pressure was normalized by dry lung weight to calculate $K_{f,c}$ value. $K_{f,c}$ was measured from the rate of lung wet weight after a step increase in venous pressure (+ 6 cmH_2O). The amount of fluid filtered in a 5 min period was determined by logarithmic extrapolation of the slower component to zero time. $K_{f,c}$ was computed in units of ml/min/cmH_2O/dry g. Lungs excised at the end of the experiment were dried in an oven at 60°C for determination of the dry lung weight. In a separate study, lungs were directly excerised and weighed for determination of final wet lung weight. The lungs were then stored in an oven at 60°C. The lungs were weighed until the dry weight was stable for longer than 5 d, to allow determination of wet/dry weight ratio.

Statistical analysis. Statistical analysis was performed using ANOVA with Fisher's PLSD post hoc test if appropriate. A value of $P < 0.05$ was considered significant.

Results

Characterization of BMPCs

Following 21 d in culture, the bone marrow-derived cells were collected for FACS analysis. These bone marrow-derived cells expressed stem/progenitor cell markers CD133 (92% ±5), Sca1 (83% ± 6), and CD34 (78% ±5) (**Supplemental Figure 1**). However, only a few bone marrow-derived cells expressed mature endothelial markers VE-cadherin and CD31 (**Supplemental Figure 1**). To further determine whether these bone marrow-derived cells are progenitor cells, we performed colony forming unit assay. As shown in **Figure 1**, there was a marked difference in the CFU-C production by the BM-derived cells compared to lung microvascular endothelial cells. 65±8 % of bone marrow-derived cells formed colonies at 18 d (**Figure lA**, **1B** and **1C**) whereas very few colonies were formed by lung microvascular endothelial cells (4±2 %). Immunocytochemistry also shows the majority of the cells from the colonies of bone marrow-derived cells expressed the stem/progenitor cell markers CD133 (**Figure 1D** and **1F**) and CD34 (**Figure 1E** and **1F**). These data demonstrated that the bone marrow-derived cells exhibit the characteristics of progenitor cells, and thereby designated as BMPCs.

BMPCs abrogate thrombin-induced decrease of endothelial TER

To assess the effects of BMPCs on thrombin-induced endothelial AJ barrier dysfunction, BMPCs were co-cultured with ECs (at ratio of 1:3) for 3 d, and then challenged with thrombin. Endothelial barrier integrity was determined by real-time measurement of transendothelial electrical resistance (TER) with the ECIS system in which ECs were grown to confluence directly on the microelectrodes (25). As shown in **Figure 2**, thrombin (1, 2, and 4 U/mL) significantly decreased TER of EC monolayers (**Figures 2A** and **2D**) whereas thrombin had no

effect on the resistance values when BMPCs alone were added to the electrodes (**Figures 2B** and **2D**). Addition of BMPCs into endothelial cells prevented the thrombin-induced decrease in TER (**Figure 2C** and **2D)**. In contrast, addition of fibroblast or non-viable BMPC (fixed with paraformaldehyde) into endothelial cells has no protective effects **(Supplemental Figure 2**). Intriguingly, transient BMPC pretreatment (as short as 30 min) could also significantly reduce thrombin-induced endothelial barrier dysfunction (**Figure 2E** and **2F**).

BMPCs prevent thrombin-induced increase in vascular permeability in mouse lungs

We studied the organ distribution of injected BMPCs and localization of BMPCs in the lung. BMPCs were mainly retained in lungs 4 d post-i.v. injection compared to other organs (**Figure 3A**). As shown in **Figure 3B**, the rhodamine-labeled BMPCs at day4 after injection were localized within lung microvessels as seen by rhodamine-labeled BMPCs surrounded by lung vascular endothelial cells stained with FITC-conjugated VE-cadherin, an endothelial cell marker.

To address the *in vivo* relevance of endothelial barrier protection induced by BMPCs, we next assessed alterations in pulmonary microvascular permeability and lung edema formation by measuring microvessel filtration coefficient ($K_{f,c}$) and lung wet weight gain in mice. Each mouse was injected i.v. (jugular vein) with 0.3 x 10^6 BMPCs or mouse lung ECs, and sacrificed 4 d after BMPC or EC injection. Mouse lungs were removed and perfused with medium with or without thrombin challenge (4 U/mL) for 15 min. BMPC transplantation prevented the thrombin-induced increase in $K_{f,c}$ seen in control and EC transplanted groups (**Figure 3C**). Lung wet/dry weight ratios were increased after challenge with thrombin in both control and EC treatment groups (**Figure 3D**), whereas edema formation was significantly reduced in BMPC-

transplanted group (**Figure 3D**). BMPC accumulation in lungs was not associated with an increase in pulmonary artery pressure (**Figures 3E** and **3F**).

BMPCs prevent VE-cadherin dissociation from plasma membrane

Since VE-cadherin homotypic adhesion is required for endothelial barrier function (9, 12, 14, 17, 20), we determined alterations in VE-cadherin distribution after the addition of rhodamine-labeled BMPCs. We observed that the characteristic time-dependent decrease in VE-cadherin staining after thrombin stimulation of ECs was inhibited by the co-culture of BMPCs (**Figure 4A**). Western blotting of VE-cadherin showed that BMPCs prevented the decrease in membrane-associated VE-cadherin typically seen after thrombin stimulation of ECs (**Figure 4B** and **4C**).

BMPCs suppress thrombin-induced RhoA activation and MLC phosphorylation

Thrombin induces formation of inter-cellular AJ gaps and actin stress fibers in ECs (3). As shown in **Figure 5A**, co-culture of BMPCs with ECs (at ratio of 1:3) significantly reduced actin polymerization and gap formation. We then assessed the amount of active monomeric GTPase RhoA (RhoA-GTP) because of its role in mediating EC actin stress fiber reorganization and inter-endothelial gap formation (1, 15). BMPCs prevented the increase in thrombin-induced RhoA activity in ECs (**Figure 5B**). As RhoA activation induces MLC phosphorylation and increases endothelial permeability (1, 7), we next examined whether BMPC-induced inhibition of RhoA interferes with MLC phosphorylation. In ECs alone, thrombin (4 U/mL for 5, 15 and 30 min) increased MLC phosphorylation (**Figure 5C**), whereas BMPCs co-cultured with ECs or addition of BMPC-conditioned media prevented the phosphorylation response (**Figure 5D** and **5E**). We also observed that BMPC-conditioned medium significantly reduced the thrombin-induced decrease in TER (**Figure 5F** and **5G**).

Endothelial barrier protection is mediated by BMPC-induced Cdc42 activation in endothelial cells

As the RhoGTPase Cdc42 is known to mediate endothelial barrier re-annealing (4, 12), we next investigated the role of Cdc42 in signaling the endothelial barrier protective effect of BMPCs. GTP-bound Cdc42 was increased within 15 min after addition of $5x10^5$ BMPCs to confluent ECs (**Figure 6A**). BMPC addition significantly increased basal TER (**Figures 6B** and **6C**). BMPC addition also induced Cdc42 activation in thrombin-challenged ECs (**Figure 6D** and **6E**). To determine if Cdc42 activation in ECs was required for BMPC-mediated endothelial barrier protection, ECs were transfected with Cdc42 siRNA to knockdown Cdc42 (**Figure 7A**) before addition of either BMPCs or ECs to the Cdc42-depleted endothelial cells (at ratio of 1:3). As shown in **Figure 7B** and **7C,** treatment of ECs with Cdc42 siRNA prevented the recovery of endothelial TER induced by BMPCs, suggesting BMPC-induced activation of Cdc42 in ECs is the critical determinant of BMPC-elicited protective effects on endothelial barrier function.

Discussion

We addressed here the effects of BMPCs in mediating endothelial barrier protection in response to thrombin challenge. We demonstrated that BMPCs added to endothelial monolayers or injected in mice prevented the increase in endothelial permeability induced by thrombin. BMPCs functioned by inhibiting the thrombin-mediated disassembly of VE-cadherin junctions. The barrier protection required BMPC-induced activation of Cdc42 in endothelial cells and attenuation of thrombin-induced RhoA activation and MLC phosphorylation. Thus, BMPCs mitigated the increase in endothelial permeability induced by thrombin by interfering directly with the mechanisms mediating the increased permeability response.

The endothelial barrier protective effect of BMPCs was established in studies in which BMPCs were added directly onto ECs. BMPCs prevented the thrombin-mediated decrease in TER and disruption of VE-cadherin junctions. In contrast, addition of ECs, fibroblast or fixed BMPCs did not have a protective effect. Endothelial barrier protection was also seen in mouse lungs as evident by measuring the pulmonary microvessel filtration coefficient ($K_{f,c}$) and wet/dry weight changes. BMPC injection significantly reduced the thrombin-induced increase in $K_{f,c}$ and lung edema formation compared to control lungs receiving ECs. The protection may be the result of the finding that ~60% of the injected BMPCs were retained in lungs. Lung BMPC uptake did not increase pulmonary artery pressure suggesting that BMPC sequestration in lungs did not induce a significant blockage of lung vessels.

Thrombin-induced increases in vascular permeability is known to be mediated by the activation of RhoA and phosphorylation of MLC leading to opening AJs (7, 9). Hence we used thrombin to test the signaling mechanism of BMPC-mediated endothelial protection. BMPCs prevented both RhoA activation and MLC phosphorylation. The protective effects of BMPCs

appeared to be due to release of secondary factors since BMPC-conditioned medium elicited the similar protective response as BMPCs. We have recently shown that BMPCs release large amounts of sphingosine -1-phosphate (31), which is known to prevent the thrombin-induced increase in endothelial permeability (13).

The actin cytoskeletal re-organization and polymerization in response to thrombin are mediated secondary to MLC phosphorylation through activation of the monomeric GTPase RhoA (1, 6). RhoA mediated-MLC phosphorylation results in formation of inter-endothelial gaps due to endothelial cell contraction (1, 7, 15, 27). We observed here that BMPC addition to EC monolayers significantly reduced thrombin-induced actin polymerization in ECs concomitant with reduced RhoA activation and MLC phosphorylation.

We have shown that activated RhoGTPase Cdc42 in contrast to RhoA signals the annealing of endothelial junctions in ECs exposed to thrombin (4, 19). This effect of Cdc42 is secondary to its role in promoting the interaction of α-catenin with β-catenin and the assembly of AJs and AJ interaction with the actin cytoskeleton (4, 12, 17). Therefore, we addressed whether BMPC addition to EC monolayers might signal AJ annealing by a similar mechanism. We observed that BMPCs increased the amount of GTP-bound Cdc42 (the active form) in control EC or thrombin-challenged ECs whereas depletion of Cdc42 prevented BMPC-mediated endothelial barrier protection. Thus, the interaction of BMPCs with ECs activates Cdc42 in ECs, and may thereby elicit the integrity of AJs. This finding is consistent with the described role of Cdc42 as an essential determinant of endothelial junction integrity (4, 12).

In summary, our results show that BMPCs prevent thrombin-mediated AJ disassembly by activating Cdc42 and inhibiting MLC phosphorylation secondary to inactivation of RhoA. These results raise the possibility that BMPC transplantation or mobilization of BMPCs can induce

endothelial barrier protection by interfering with signaling pathways in ECs mediating the increased permeability in response to pro-inflammatory mediators.

Acknowledgments

This research was supported by NIH grants R01 HL 085462 (Y.Y.Z), and R01 HL090152 (A.B.M), and the grant from Illinois Stem Cell Research Program (A.B.M). H.O. was supported in part by the Banyu Fellowship Program of Banyu Life Science Foundation International. The authors would like to thank Dr. Kelly Price for her critical reading. We also thank Qiyan Zhou and Nanjia Yu for their expert technical assistance.

References

1. **Amano M, Chihara K, Kimura K, Fukata Y, Nakamura N, Matsuura Y, and Kaibuchi K**. Formation of actin stress fibers and focal adhesions enhanced by Rho-kinase. *Science* 275: 1308-1311, 1997.
2. **Asahara T, Murohara T, Sullivan A, Silver M, van der Zee R, Li T, Witzenbichler B, Schatteman G, and Isner JM**. Isolation of putative progenitor endothelial cells for angiogenesis. *Science* 275: 964-967, 1997.
3. **Birukova AA, Smurova K, Birukov KG, Kaibuchi K, Garcia JG, and Verin AD**. Role of Rho GTPases in thrombin-induced lung vascular endothelial cells barrier dysfunction. *Microvasc Res* 67: 64-77, 2004.
4. **Broman MT, Kouklis P, Gao X, Ramchandran R, Neamu RF, Minshall RD, and Malik AB**. Cdc42 regulates adherens junction stability and endothelial permeability by inducing alpha-catenin interaction with the vascular endothelial cadherin complex. *Circ Res* 98: 73-80, 2006.
5. **Cooper JA, Lo SK, and Malik AB**. Fibrin is a determinant of neutrophil sequestration in the lung. *Circ Res* 63: 735-741, 1988.
6. **Coughlin SR**. Thrombin signalling and protease-activated receptors. *Nature* 407: 258-264, 2000.
7. **Garcia JG, Davis HW, and Patterson CE**. Regulation of endothelial cell gap formation and barrier dysfunction: role of myosin light chain phosphorylation. *J Cell Physiol* 163: 510-522, 1995.
8. **Gupta N, Su X, Popov B, Lee JW, Serikov V, and Matthay MA**. Intrapulmonary delivery of bone marrow-derived mesenchymal stem cells improves survival and attenuates endotoxin-induced acute lung injury in mice. *J Immunol* 179: 1855-1863, 2007.
9. **Iyer S, Ferreri DM, DeCocco NC, Minnear FL, and Vincent PA**. VE-cadherin-p120 interaction is required for maintenance of endothelial barrier function. *Am J Physiol Lung Cell Mol Physiol* 286: L1143-1153, 2004.
10. **Kawamoto A, Gwon HC, Iwaguro H, Yamaguchi JI, Uchida S, Masuda H, Silver M, Ma H, Kearney M, Isner JM, and Asahara T**. Therapeutic potential of ex vivo expanded endothelial progenitor cells for myocardial ischemia. *Circulation* 103: 634-637, 2001.
11. **Kocher AA, Schuster MD, Szabolcs MJ, Takuma S, Burkhoff D, Wang J, Homma S, Edwards NM, and Itescu S**. Neovascularization of ischemic myocardium by human bone-marrow-derived angioblasts prevents cardiomyocyte apoptosis, reduces remodeling and improves cardiac function. *Nat Med* 7: 430-436, 2001.
12. **Kouklis P, Konstantoulaki M, and Malik AB**. VE-cadherin-induced Cdc42 signaling regulates formation of membrane protrusions in endothelial cells. *J Biol Chem* 278: 16230-16236, 2003.
13. **Kouklis P, Konstantoulaki M, Vogel S, Broman M, and Malik AB**. Cdc42 regulates the restoration of endothelial barrier function. *Circ Res* 94: 159-166, 2004.
14. **Lampugnani MG, Corada M, Caveda L, Breviario F, Ayalon O, Geiger B, and Dejana E**. The molecular organization of endothelial cell to cell junctions: differential association of plakoglobin, beta-catenin, and alpha-catenin with vascular endothelial cadherin (VE-cadherin). *J Cell Biol* 129: 203-217, 1995.
15. **Mehta D, Ahmmed GU, Paria BC, Holinstat M, Voyno-Yasenetskaya T, Tiruppathi C, Minshall RD, and Malik AB**. RhoA interaction with inositol 1,4,5-trisphosphate receptor and

transient receptor potential channel-1 regulates Ca2+ entry. Role in signaling increased endothelial permeability. *J Biol Chem* 278: 33492-33500, 2003.
16. **Mei SH, McCarter SD, Deng Y, Parker CH, Liles WC, and Stewart DJ**. Prevention of LPS-induced acute lung injury in mice by mesenchymal stem cells overexpressing angiopoietin 1. *PLoS Med* 4: e269, 2007.
17. **Navarro P, Ruco L, and Dejana E**. Differential localization of VE- and N-cadherins in human endothelial cells: VE-cadherin competes with N-cadherin for junctional localization. *J Cell Biol* 140: 1475-1484, 1998.
18. **Rafii S, and Lyden D**. Therapeutic stem and progenitor cell transplantation for organ vascularization and regeneration. *Nat Med* 9: 702-712, 2003.
19. **Ramchandran R, Mehta D, Vogel SM, Mirza MK, Kouklis P, and Malik AB**. Critical role of Cdc42 in mediating endothelial barrier protection in vivo. *Am J Physiol Lung Cell Mol Physiol* 295: L363-369, 2008.
20. **Sandoval R, Malik AB, Minshall RD, Kouklis P, Ellis CA, and Tiruppathi C**. Ca(2+) signalling and PKCalpha activate increased endothelial permeability by disassembly of VE-cadherin junctions. *J Physiol* 533: 433-445, 2001.
21. **Schmidt-Lucke C, Rossig L, Fichtlscherer S, Vasa M, Britten M, Kamper U, Dimmeler S, and Zeiher AM**. Reduced number of circulating endothelial progenitor cells predicts future cardiovascular events: proof of concept for the clinical importance of endogenous vascular repair. *Circulation* 111: 2981-2987, 2005.
22. **Shintani S, Murohara T, Ikeda H, Ueno T, Honma T, Katoh A, Sasaki K, Shimada T, Oike Y, and Imaizumi T**. Mobilization of endothelial progenitor cells in patients with acute myocardial infarction. *Circulation* 103: 2776-2779, 2001.
23. **Szmitko PE, Fedak PW, Weisel RD, Stewart DJ, Kutryk MJ, and Verma S**. Endothelial progenitor cells: new hope for a broken heart. *Circulation* 107: 3093-3100, 2003.
24. **Takahashi T, Kalka C, Masuda H, Chen D, Silver M, Kearney M, Magner M, Isner JM, and Asahara T**. Ischemia- and cytokine-induced mobilization of bone marrow-derived endothelial progenitor cells for neovascularization. *Nat Med* 5: 434-438, 1999.
25. **Tiruppathi C, Malik AB, Del Vecchio PJ, Keese CR, and Giaever I**. Electrical method for detection of endothelial cell shape change in real time: assessment of endothelial barrier function. *Proc Natl Acad Sci U S A* 89: 7919-7923, 1992.
26. **Tiruppathi C, Song W, Bergenfeldt M, Sass P, and Malik AB**. Gp60 activation mediates albumin transcytosis in endothelial cells by tyrosine kinase-dependent pathway. *J Biol Chem* 272: 25968-25975, 1997.
27. **van Nieuw Amerongen GP, Draijer R, Vermeer MA, and van Hinsbergh VW**. Transient and prolonged increase in endothelial permeability induced by histamine and thrombin: role of protein kinases, calcium, and RhoA. *Circ Res* 83: 1115-1123, 1998.
28. **Vogel SM, Gao X, Mehta D, Ye RD, John TA, Andrade-Gordon P, Tiruppathi C, and Malik AB**. Abrogation of thrombin-induced increase in pulmonary microvascular permeability in PAR-1 knockout mice. *Physiol Genomics* 4: 137-145, 2000.
29. **Yoder MC, Mead LE, Prater D, Krier TR, Mroueh KN, Li F, Krasich R, Temm CJ, Prchal JT, and Ingram DA**. Redefining endothelial progenitor cells via clonal analysis and hematopoietic stem/progenitor cell principals. *Blood* 109: 1801-1809, 2007.
30. **Zhao YD, Courtman DW, Deng Y, Kugathasan L, Zhang Q, and Stewart DJ**. Rescue of monocrotaline-induced pulmonary arterial hypertension using bone marrow-derived endothelial-like progenitor cells: efficacy of combined cell and eNOS gene therapy in established

disease. *Circ Res* 96: 442-450, 2005.
31. **Zhao YD, Ohkawara H, Rehman J, Wary KK, Vogel SM, Minshall RD, Zhao YY, and Malik AB**. Bone marrow progenitor cells induce endothelial adherens junction integrity by sphingosine-1-phosphate-mediated Rac1 and Cdc42 signaling. *Circ Res* 105: 696-704, 2009.

Figure Legends

Figure 1. BMPCs exhibit the characteristics of progenitor cells. (**A-C**) Colony forming unit assays demonstrating the progenitor potential of BMPCs. BMPCs or mouse lung ECs were plated at a density of 10^3 cells/well of 6-well plate with MethodCult RH4100 mixed with EBM-2MV medium (1:1) containing 5% FBS. Following 18 d in culture, the colonies formed in collagen gels were counted. Data are expressed as mean ± SD (n=3 experiments). *, $P < 0.001$ versus EC (**A**). Representative micrographs showing the colonies formed by BMPCs (**B, C**). Scale bar, 100μm. (**D-F)** The majority of BMPCs expressed the stem/progenitor cell markers CD133 and CD34. At the end of the 18d clonogenic assay, the cells were collected and re-plated on Chamber slides. Following 2 d in culture, the cells were then fixed in 4% paraformaldehyde and immunostained with antibodies against CD133 or CD34 (green). Nuclei were counterstained with DAPI (blue). Representative micrographs of immunostaining of CD133 (**D**) or CD34 (**E**) are shown. Scale bar, 100μm. The percentage of CD133+ or CD34+ BMPCs was quantified (**F**). Data are expressed as mean ± SD (n=3 experiments).

Figure 2. BMPCs prevent endothelial barrier dysfunction induced by thrombin. (A-D) The effects of 3d co-culture of BMPCs with ECs on endothelial barrier function in response to thrombin. Real-time changes in TER in response to thrombin (1, 2 and 4 U/mL) were monitored in mouse lung EC cultures (**A**), BMPC cultures (**B**), or the 3d EC-BMPC co-cultures (at ratio of 3:1) (**C**). Data are representative of 3 experiments. The maximal changes in TER were quantified (**D).** Data are expressed as mean ± SD (n=3). $^*P < 0.05$. Throm, thrombin. (**E-F**) The effects of transient BMPC treatment on endothelial barrier function in response to thrombin. BMPCs were added to endothelial monolayers at the indicated times prior to thrombin challenge

(4U/ml), and real-time changes in TER were then monitored for 4h (**E**). Data are representative of 3 experiments. The maximal changes in TER were quantified (**F).** Data are expressed as mean ± SD (n=3). $^{*}P < 0.05$ versus EC treated with thrombin. 30 min pretreatment of BMPCs significantly attenuated thrombin-induced endothelial barrier dysfunction.

Figure 3. Lung uptake of BMPCs and BMPC-mediated prevention of thrombin-induced increase in lung vascular permeability. (A) BMPC uptake in lungs. $3x10^5$ BMPCs labeled with ^{111}Indium oxine were injected into each mouse through jugular vein. Approximately 60% of the injected BMPCs were retained in lungs 4d post-injection. Data are expressed as mean ± SD (n= 5 mice). (**B**) Representative micrographs of fluorescent staining demonstrating BMPC localization within lung microvessels. 4d post-injection of rhodamine-labeled BMPCs ($3x10^5$ cells/mouse through the external jugular vein), cryosections of lung tissues were used for assessment of BMPCs localization (red). Lung vascular endothelial cells were immunostained with anti-VE-cadherin (green) and nuclei were counterstained with DAPI (blue). Arrows indicate the rhodamine-labeled BMPCs surrounded by lung vascular endothelial cells. Scale bar, 50μm. (**C)** Effects of BMPCs on pulmonary microvascular hyper-permeability response to thrombin. 4d post-BMPC or mouse lung EC injection (via external jugular vein), the mouse lungs were isolated and perfused for 15 min using RPMI1640 medium with or without 4 U/ml of thrombin. Pulmonary microvessel filtration coefficient ($K_{f,c}$) was then measured to determine pulmonary microvascular permeability. Data are expressed as mean ± SD (n = 5). *, $P < 0.05$. BMPC transplantation prevented the thrombin-induced increase in $K_{f,c}$ whereas EC transplantation had no effect. (**D)** Effect of BMPCs on thrombin-induced lung edema formation determined by measuring lung water content. Data are expressed as mean ± SD (n = 5). *, $P < 0.05$. In the BMPC treatment group following thrombin challenge, lung wet/dry weight ratio was decreased

compared with control groups injected with or without mouse lung ECs. (**E-F)** Injection of either BMPCs or ECs did not significantly change pulmonary artery pressure (Ppa) (**E**) and delta pulmonary artery pressure (delta Ppa) (**F**). Data are expressed as mean ± SD (n=5). ns, not significant.

Figure 4. BMPCs retain VE-cadherin in plasma membrane following thrombin challenge. **(A**) Representative micrographs of VE-cadherin immunostaining demonstrating BMPCs prevented thrombin-induced decrease of VE-cadherin expression in plasma membrane. Confluent mouse lung EC cultures or EC-BMPC co-cultures at 3d were challenged with thrombin (4 U/mL) for the indicated times. The fixed cells were immunostained with anti-VE-cadherin antibody (green). Nuclei were counterstained with DAPI (blue). Scale bar, 50 μm. (**B-C**) Translocation of VE-cadherin in response to thrombin determined by Triton X-100 solubility assay. Cells were stimulated with thrombin (4 U/mL) for the times indicated (10, 30, and 60 min), and fractionated with cytoskeleton-stabilizing buffer. Representative immunoblots of anti-VE-cadherin from three similar experiments are shown. Bar graphs show quantitative densitometric analysis of each band. Data are expressed as mean ± SD (n=3 experiments). *, $P < 0.05$ versus control. BMPC treatment inhibited thrombin-induced dissociation of VE-cadherin from plasma membrane.

Figure 5. BMPCs inhibit thrombin-induced RhoA activation and MLC phosphorylation. **(A)** Actin stress fiber distribution in ECs cultured with or without BMPCs basally or following thrombin challenge (4U/ml). ECs were co-cultured with BMPCs (at ratio of 3:1) for 3d prior to thrombin challenge. Fluorescent staining was performed using FITC-conjugated phalloidin (green). Nuclei were counterstained with DAPI (blue). Representative fluorescent images from three experiments are shown. Scale bar, 50 μm. (**B)** Effect of BMPCs on thrombin-induced

RhoA activation. ECs were co-cultured with BMPCs (at ratio of 3:1) for 3d before addition of thrombin (4 U/ml). Pull-down assays were performed to determine GTP-bound RhoA (active form) (GTP-RhoA). Representative immunoblots of anti-RhoA antibody from three experiments are shown in the top panel. The intensity of each band was quantified and Data are expressed as mean ± SD (n=3). *, $P < 0.05$ versus EC-BMPC co-culture treated with thrombin. (**C-E)** Effect of BMPCs on MLC phosphorylation in response to thrombin. ECs were co-cultured with BMPCs (at ratio of 3:1) for 3 d before thrombin (4 U/ml) was added. 5 min post-thrombin challenge, MLC phosphorylation was assessed by immunoblotting using an antibody specific for phosphorylated MLC (MLCp). Representative immunoblots from 3 experiments are shown. Data are expressed as mean ± SD (n=3). *, $P < 0.05$ versus control EC (**C**). BMPC treatment suppressed thrombin-induced MLC phosphorylation in mouse lung EC (**D**). BMPC-conditioned medium (CM) significantly reduced thrombin-induced increase in endothelial MLC phosphorylation (**E**). *, $P < 0.05$ versus control. **(F-G)** TER assay demonstrating treatment with BMPC-conditioned medium reduced thrombin-induced increase in endothelial permeability. Representative real-time TER measurements of 3 experiments are shown (**F**). Peak TER changes were presented by bar graphs (**G**). Data are expressed as mean ± SD (n=3 experiments). *, $P < 0.05$. **, $P < 0.01$.

Figure 6. BMPCs induce Cdc42 activation in endothelial cells. (**A)** Effect of BMPCs on Cdc42 activity determined by level of CdC42-GTP. Following BMPCs (50,000 cells per 60mm dish) addition to confluent mouse lung EC monolayer, the cells were lysed at indicated times. Pull-down assays were performed to determine the GTP-bound active Cdc42 (GTP-Cdc42). Data are expressed as mean ± SD from three independent experiments. *, $P < 0.05$ versus control (0 min). **(B-C)** Effects of BMPCs on endothelial barrier function basally. TER was measured in

pulmonary microvessel endothelial monolayers to which BMPCs or ECs (5000 cells/per well) were added. Data are representative of three experiments. *, $P < 0.05$ versus controls with/out addition of EC. (**D)** Effects of BMPCs on Cdc42 activity in response to thrombin challenge. 5min post-thrombin challenge (4U/mL), BMPCs were added to EC monolayer. Cdc42 activity was then determined by the amount of Cdc42-GTP at 15 min after addition of BMPC. Bars are mean ± SD of quantitative densitometric analysis from three experiments. $^{*}P < 0.05$ versus control. Throm, thrombin. (**E**) Effects of BMPCs on Cdc42 activity in thrombin-challenged ECs determined by immnofluorescence staining. BMPCs were added to ECs 5 min after thrombin challenge (4 U/mL), and cells were fixed 20 min after thrombin challenge. Cdc42 were stained with anti-Cdc42 antibody (green) and nuclei were counterstained with DAPI (blue). Representative fluorescent images of three experiments are shown. Arrows indicate BMPCs-induced membrane expression of Cdc42. Scale bar, 50 μm.

Figure 7. Endothelial barrier protection is mediated by BMPC-induced Cdc42 activation in endothelial cells. (**A)** Western blotting demonstrating siRNA-mediated knockdown of Cdc42 in mouse lung ECs. Densitometry from immunoblots showed Cdc42 protein expression was efficiently reduced 72 h after transfection. *, $P < 0.01$ versus control siRNA-transfected ECs (n=3 experiments). (**B-C**) TER assay demonstrating BMPC inhibition of thrombin-induced endothelial barrier dysfunction was mediated by Cdc42 activation in ECs. ECs were transfected with either Cdc42 siRNA or scrambled control siRNA. 4h post-transfection, BMPCs were added to the EC cultures (BMPCs:ECs, 1:3). 72h post-transfection, thrombin (4U/ml) were added to the cultures and TER was monitored to assess the endothelial barrier function (**B**). Data are representative of four independent experiments. Data of maximal TER changes are expressed as mean ± SD (**C**). *, $P < 0.01$.

Supplemental Figure Legends

Supplemental Figure 1. FACS analysis of BMPCs demonstrating that greater than 90% of BMPCs express the progenitor cell markers. FACS analysis was made using cultured BMPCs on day21 to assess surface expression of the hematopoietic progenitor/stem cell markers (CD133, CD34, Sca1) and mature endothelial cell markers (VE-cadherin and CD31). Three independent BMPC preparations were characterized by FACS analysis. Data are expressed as mean ± SD.

Supplemental Figure 2. The effects of fibroblasts and fixed BMPCs on thrombin-induced endothelial barrier dysfunction. BMPCs, fibroblasts and non-viable BMPC (fixed in paraformaldehyde) were co-cultured with ECs (at ratio of 1:3) for 3d prior to thrombin stimulation, and changes in TER were measured up to 4h. Representative TER measurements of three experiments are shown (**A**). Data of maximal TER changes are expressed as mean ± SD (n=3) (**B**). *, $P < 0.01$. In contrast to BMPCs, mouse lung fibroblasts or non-viable BMPCs failed to preserve the endothelial barrier function in response to thrombin challenge (4U/mL).

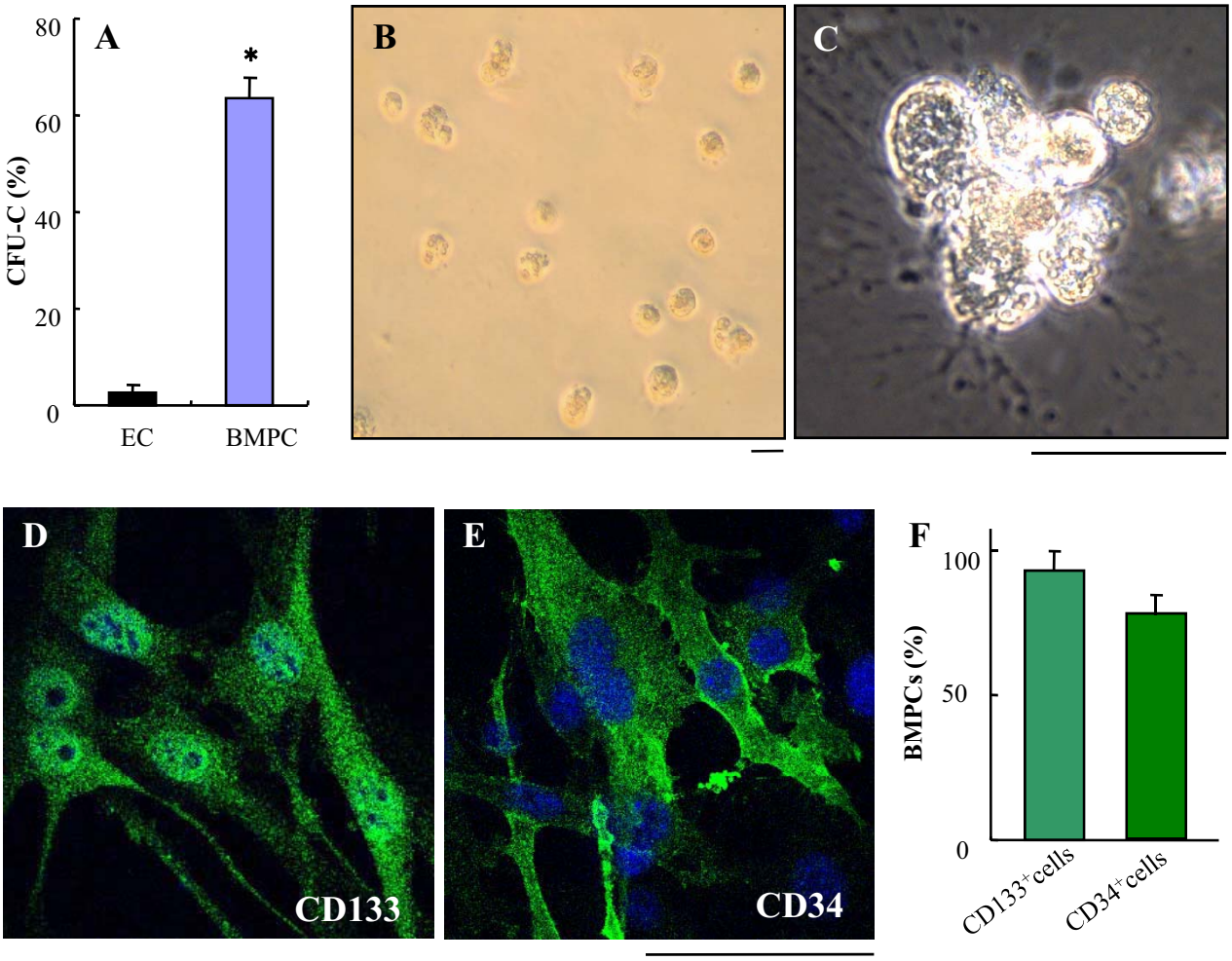
A
80
60
40
20
0
CFU-C (%)
*
EC
BMPC
B
C
D
CD133
E
CD34
F
100
50
0
BMPCs (%)
CD133+cells
CD34+cells

Figure 1

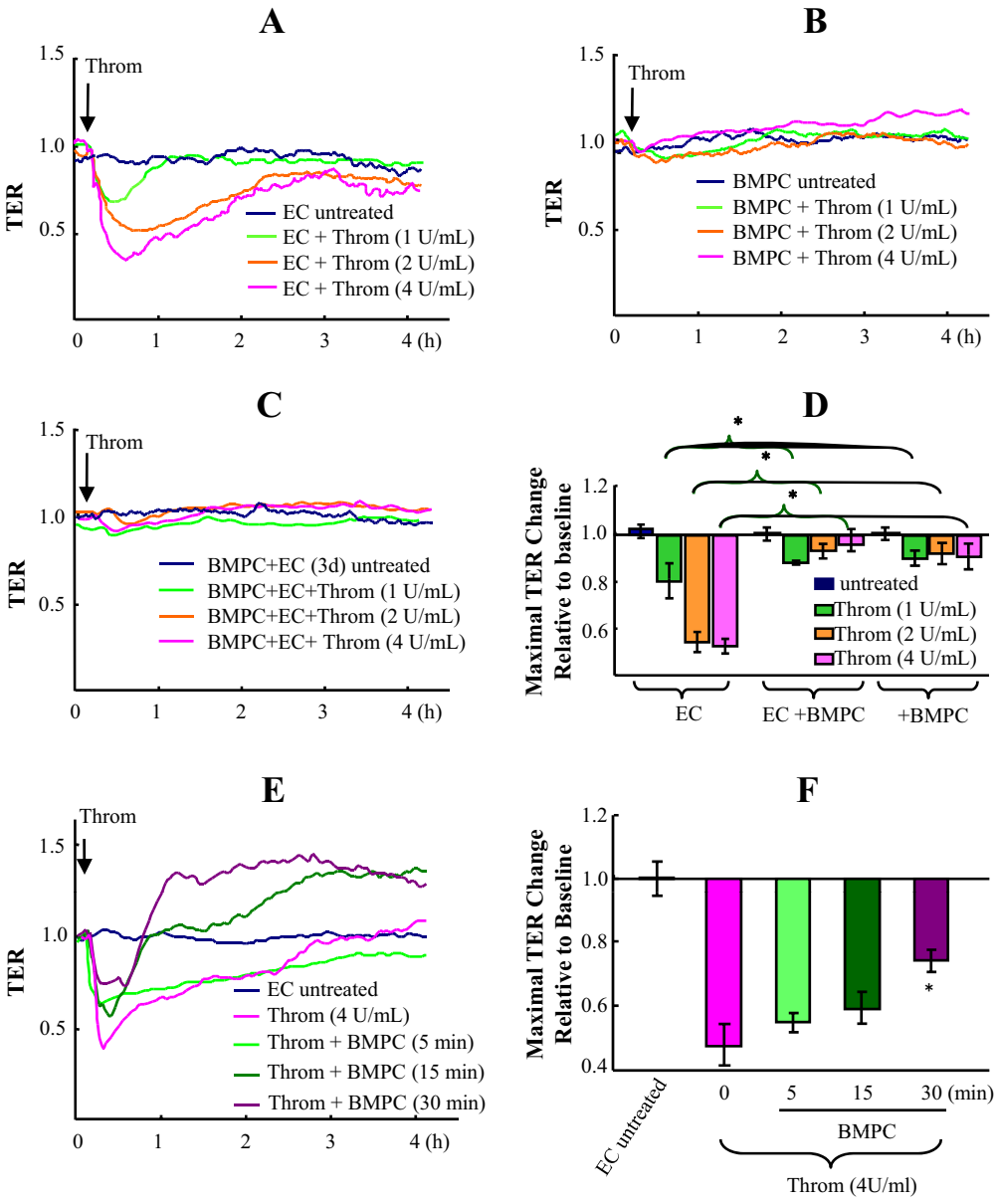
A
Throm
TER
EC untreated
EC + Throm (1 U/mL)
EC + Throm (2 U/mL)
EC + Throm (4 U/mL)
B
Throm
TER
BMPC untreated
BMPC + Throm (1 U/mL)
BMPC + Throm (2 U/mL)
BMPC + Throm (4 U/mL)
C
Throm
TER
BMPC+EC (3d) untreated
BMPC+EC+Throm (1 U/mL)
BMPC+EC+Throm (2 U/mL)
BMPC+EC+ Throm (4 U/mL)
D
Maximal TER Change
Relative to baseline
untreated
Throm (1 U/mL)
Throm (2 U/mL)
Throm (4 U/mL)
EC
EC +BMPC
+BMPC
E
Throm
TER
EC untreated
Throm (4 U/mL)
Throm + BMPC (5 min)
Throm + BMPC (15 min)
Throm + BMPC (30 min)
F
Maximal TER Change
Relative to Baseline
EC untreated
0
5
15
30 (min)
BMPC
Throm (4U/ml)

Figure 2

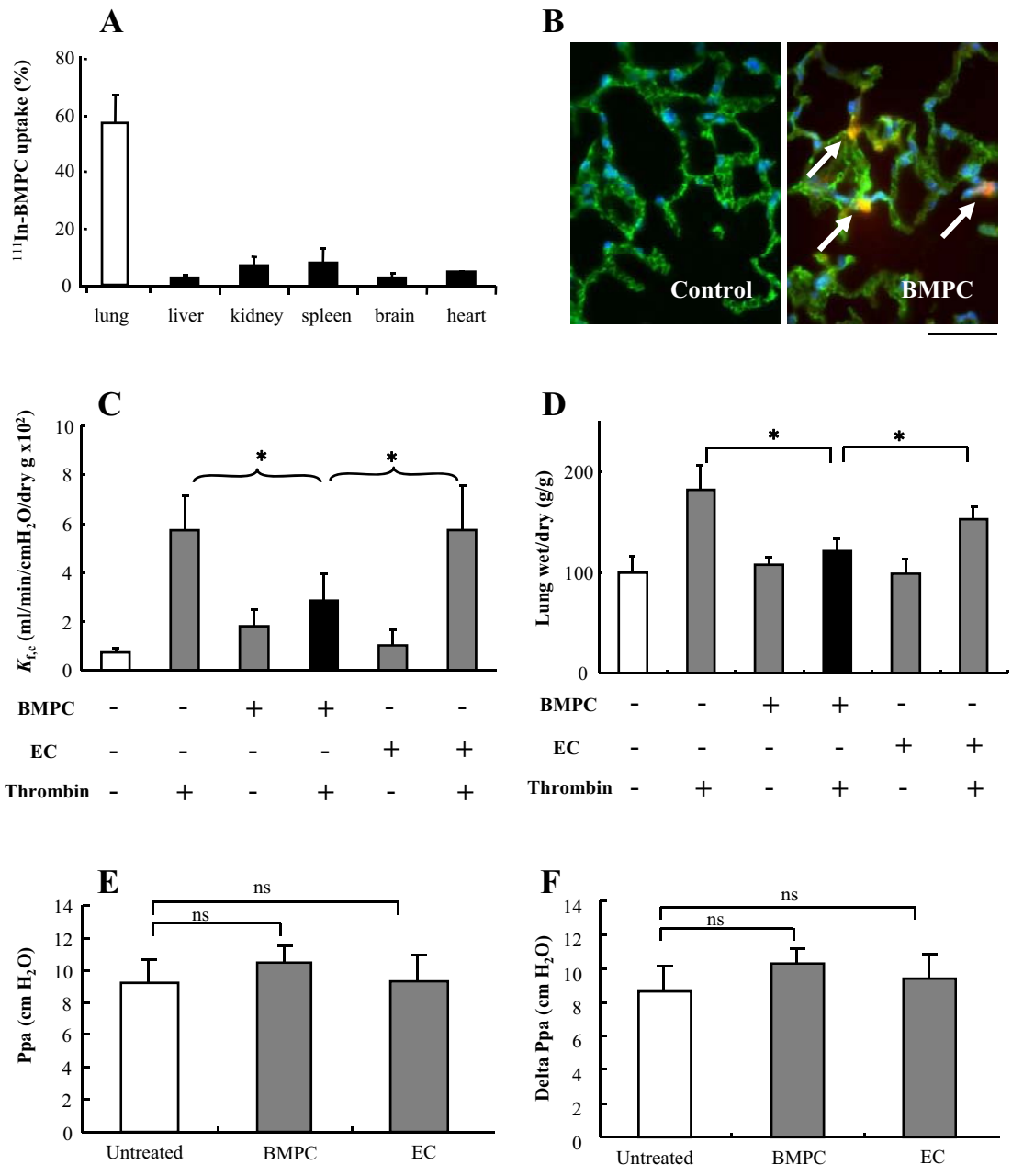
A
^{111}In-BMPC uptake (%)
80
60
40
20
0
lung
liver
kidney
spleen
brain
heart
B
Control
BMPC
C
$K_{f,c}$ (ml/min/cmH$_2$O/dry g x10^2)
10
8
6
4
2
0
*
*
BMPC - - + + - -
EC - - - - + +
Thrombin - + - + - +
D
Lung wet/dry (g/g)
200
100
0
*
*
BMPC - - + + - -
EC - - - - + +
Thrombin - + - + - +
E
Ppa (cm H$_2$O)
14
12
10
8
6
4
2
0
ns
ns
Untreated
BMPC
EC
F
Delta Ppa (cm H$_2$O)
14
12
10
8
6
4
2
0
ns
ns
Untreated
BMPC
EC

Figure 3

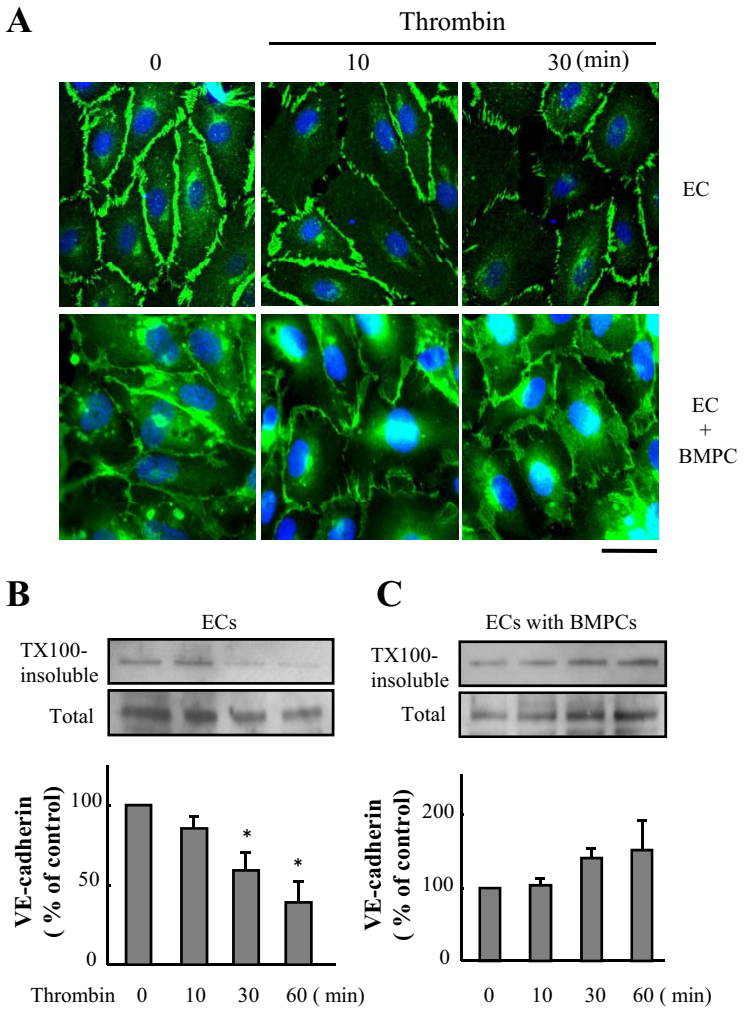
A
Thrombin
0
10
30 (min)
EC
EC
+
BMPC
B
ECs
TX100-
insoluble
Total
VE-cadherin
(% of control)
100
50
0
*
*
Thrombin 0 10 30 60 (min)
C
ECs with BMPCs
TX100-
insoluble
Total
VE-cadherin
(% of control)
200
100
0
0 10 30 60 (min)

Figure 4

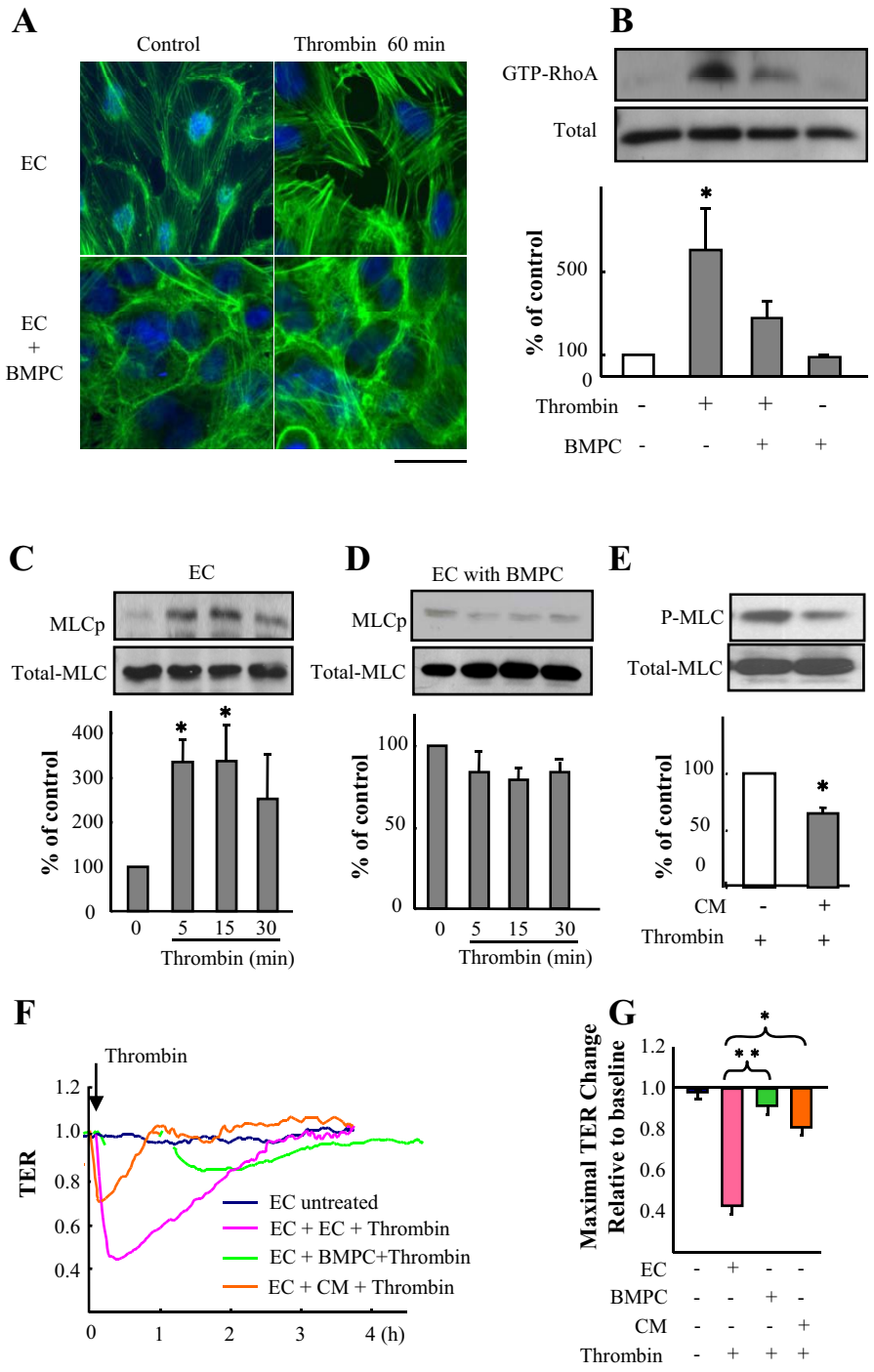
A
Control
Thrombin 60 min
EC
EC + BMPC
B
GTP-RhoA
Total
% of control
500
100
0
Thrombin - + + -
BMPC - - + +
C
EC
MLCp
Total-MLC
% of control
400
300
200
100
0
0 5 15 30
Thrombin (min)
D
EC with BMPC
MLCp
Total-MLC
% of control
100
50
0
0 5 15 30
Thrombin (min)
E
P-MLC
Total-MLC
% of control
100
50
0
CM - +
Thrombin + +
F
Thrombin
TER
1.2
1.0
0.8
0.6
0.4
0 1 2 3 4 (h)
EC untreated
EC + EC + Thrombin
EC + BMPC+Thrombin
EC + CM + Thrombin
G
Maximal TER Change Relative to baseline
1.2
1.0
0.8
0.6
0.4
EC - + - -
BMPC - - + -
CM - - - +
Thrombin - + + +

Figure 5

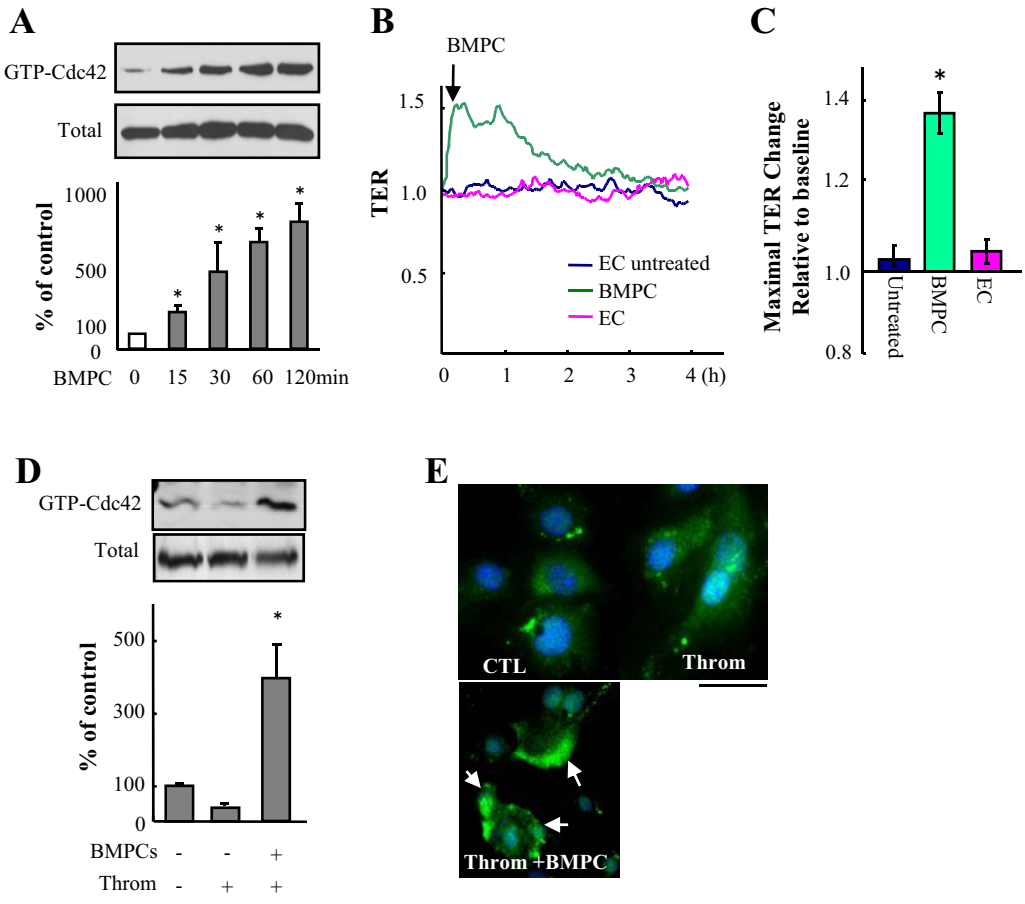
A
GTP-Cdc42
Total
% of control
1000
500
100
0
BMPC 0 15 30 60 120min
B
BMPC
TER
1.5
1.0
0.5
EC untreated
BMPC
EC
0 1 2 3 4 (h)
C
Maximal TER Change
Relative to baseline
1.4
1.2
1.0
0.8
Untreated
BMPC
EC
D
GTP-Cdc42
Total
% of control
500
300
100
0
BMPCs - - +
Throm - + +
E
CTL
Throm
Throm +BMPC

Figure 6

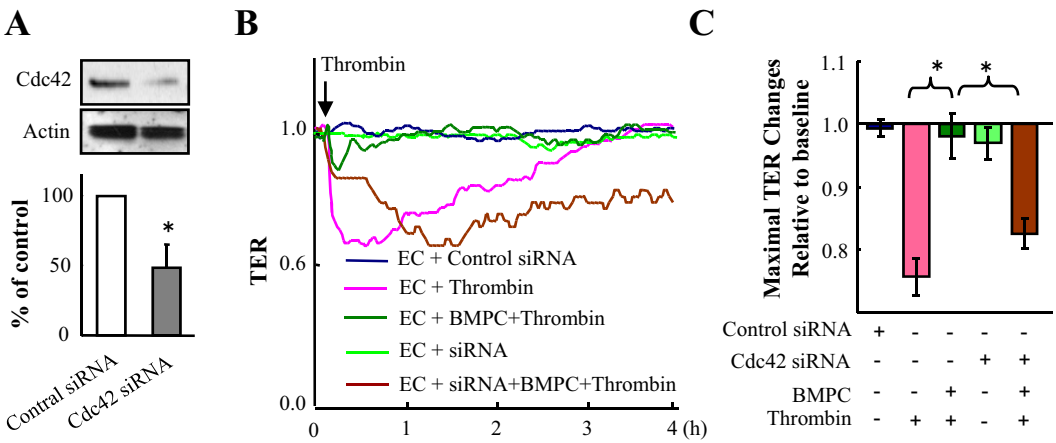
A
Cdc42
Actin
% of control
100
50
0
*
Contral siRNA
Cdc42 siRNA
B
Thrombin
TER
1.0
0.6
0.0
0
1
2
3
4 (h)
EC + Control siRNA
EC + Thrombin
EC + BMPC+Thrombin
EC + siRNA
EC + siRNA+BMPC+Thrombin
C
Maximal TER Changes
Relative to baseline
1.1
1.0
0.9
0.8
*
*
Control siRNA + - - - -
Cdc42 siRNA - - - + +
BMPC - - + - +
Thrombin - + + - +

Figure 7

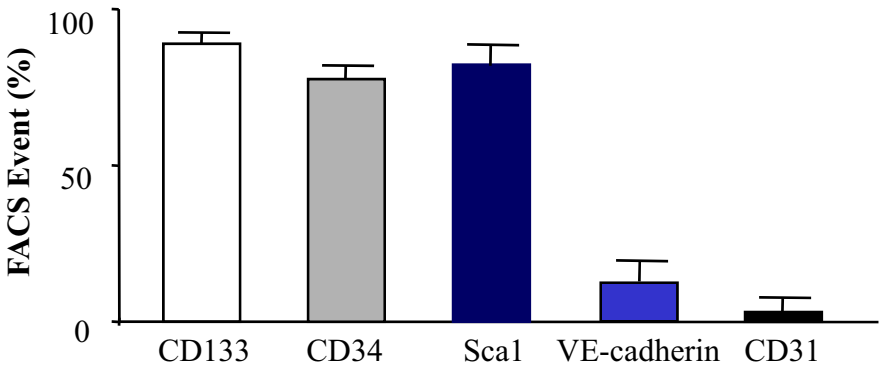

Supplemental Figure 1

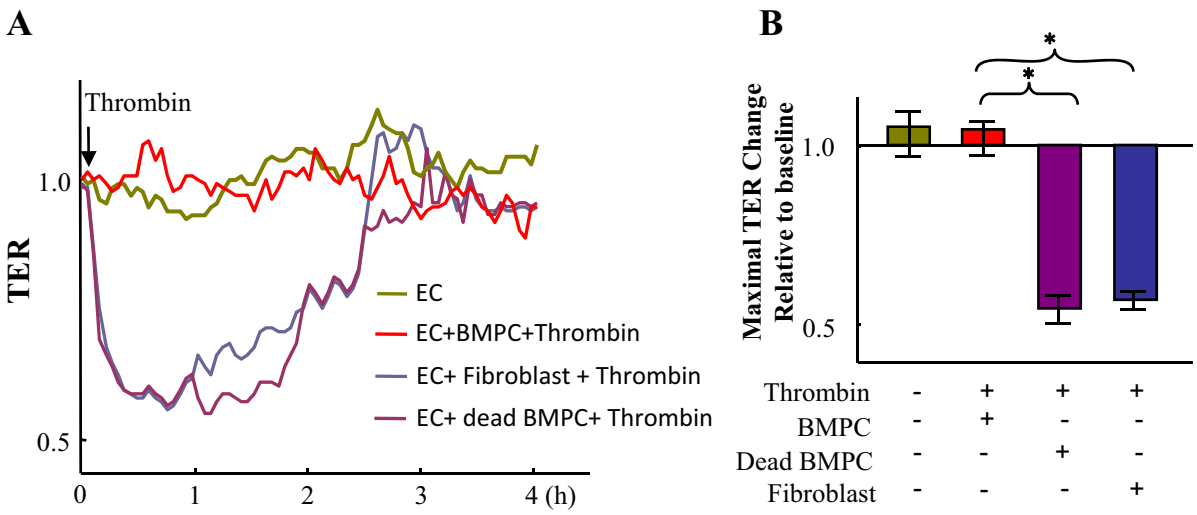

Supplemental Figure 2